Journal of the Korean Nuclear Society
Volume 5, Number 1, March, 1973

≪Original≫

Frequency Characteristics of Anodic Oxide Films on Tantalum

Dong Nyung Lee

physical Metallurgy Laboratory, Korea Institute of Science and Technology, Seoul, Korea

Yong Ku Yoon

Atomic Energy Research Institute, Seoul, Korea

(Received January 19, 1973)

Abstract

The Nishitani's equations for impedance of anodic oxide films have been derived based on a p-i-n model under the assumption of $\omega\varepsilon\rho_0 \ll 4\pi \ll \omega\varepsilon\rho_w$, where ω is angular frequency, ε is dielectric constant, and ρ_0 and ρ_w are the resistivity of the interface region and the intrisic region of the anodic oxide film, respectively. Since it is not possible to evaluate all parameters in the equations, however, any clear physical picture cannot be obtained from the equations. Therefore, the equations are modified under the assumption of $\omega\tau_w \gg 1$ and $\ln(1+\omega^2\tau_0^2) \ll 1$, where $\tau_w=\varepsilon\rho_w/(4\pi)$ and $\tau_0=\varepsilon\rho_0/(4\pi)$. The modified equations are then used to explain the change in the frequency characteristics of anodic oxide films when they are heated.

The change in impedance of anodic oxide films when they are heated is attributed mainly to the increase in the diffusion layer and to the decrease in the resistivity of anodic oxide films.

요 약

양극산화 피막의 임피단스(impedance)에 대한 니시다니(西谷)식은 p-i-n 모델에 기초를 두고 $\omega\varepsilon\rho_0 \ll 4\pi \ll \omega\varepsilon\rho_w$의 가정하에서 유도된 것이다. 여기서 ω는 각 주파수, ε는 유전상수, ρ_0와 ρ_w는 양극산화피막의 계면과 중간영역의 비저항이다. 그러나 이 식의 파라메타를 전부 계산할 수 없기 때문에 이 식으로 양극산화피막의 물리적 모형을 분명히 할 수가 없다. 그러므로 $\omega\tau_w \gg 1$과 $\ln(1+\omega^2\tau_0^2) \ll 1$이란 가정을 하여 임피단스에 대한 수정된 식을 유도하였다. 여기서 $\tau_w=\varepsilon\rho_w/(4\pi)$ 및 $\tau_0=\varepsilon\rho_0/(4\pi)$로 정의된다. 양극산화피막을 가열하였을 때의 주파수특성의 변화를 이 수정된 식으로 설명하였다.

양극산화피막을 가열하였을 때 양극산화피막의 임피단스의 변화는 주로 양극산화피막의 확산층의 증가와 비저항의 감소때문이라고 해석하였다.

1. Introduction

Anodic oxide films on valve metals, especially aluminum and tantalum, are used as dielectric of electrolytic capacitors[1,2]. Since the anodic oxide films have an effect on the electrical properties of capacitors. there have been many attempts to explain their properties. Recently, Nishitani[1] derived the equations (Eqs. 14 and 15) for equivalent series resistance and capacitance by applying the versions of Scholte[2], Sasaki[3] and Young[4]. However, Nishitani failed to determine the values of all the parameters in the equations. It was, therefore, impossible to test the assumptions he made.

This paper presents modified forms of Nishitani's equations and a method of evaluating parmeters in the equations. The equations are then used to explain the change in the impedance of anodic oxide films on tantalm before and after their heat treatment.

2. Equations for Impedance of Anodic Oxide Films

The p-i-n structure model of anodic oxde films on valve metals has been suggested by many authors[1-4]. Scholte and van Geel[2] analyzed their measurements of equivalent series resistance R_s and capacitance C_s of the |aluminum|aluminum oxide|electrolyte|system in terms of a series of parallel resistance-capacitance combinations.

$$R_s=\Sigma_i \frac{R_i}{1+\omega^2 R_i^2 C_i^2} \quad (i=1,2,\cdots) \qquad (1)$$

$$\frac{1}{C_s}=\Sigma_i \frac{\omega^2 R_i^2 C_i}{1+\omega^2 R_i^2 C_i^2} \quad (i=1,2,\cdots) \qquad (2)$$

where R_i and C_i are the components of the ith parallel combination and $\omega=2\pi f$ (f is frequency). Here R_i and C_i are assumed to be independent of frequency.

Impedance measurements on anodic oxide films on niobium by Young[4] showed that plots of $1/C_s$ against log f and plots of R_s against $1/f$ were linear; and the ratio of the slopes of the plots was close to 9.2~4 ln 10.

The result could be accounted for by considering that the frequency dependence of the film impedance is due to a variation in conductivity through the film, as can be seen from the Scholte and van Geel's theory described in the following: Consider an infinitesimal sheet element of oxide of thickness dx, resistance dR and capacity dC at a distance from the metal. This element contributes $dR/[1+\omega^2(dC)^2(dR)^2]$ and $\omega^2(dR)^2dC/[1+\omega^2(dR)^2(dC)^2]$ to the equivalent series resistance R_f and to reciprocal of the equivalent series capacitance $1/C_f$ as in Eqs. (1) and (2)*

$$R_f=\int_0^d \frac{dR}{1+\omega^2(dC)^2(dR)^2} \qquad (3)$$

$$\frac{1}{C_f}=\int_0^d \frac{\omega^2(dR)^2dC}{1+\omega^2(dR)^2(dC)^2} \qquad (4)$$

where d is the film thickness. The resistance dR and the capacity dC can be expressed by

$$dR=\rho(x)\frac{dx}{A}$$

and $$dC=\frac{\kappa A}{dx}$$

Here $\rho(x)$ is the resistivity at distance x from the metal/oxide interface into the oxide, A is the area of the film, and

$\kappa=\varepsilon/(4\pi\times9\times10^{11})=0.0885\times10^{-12}\varepsilon$ farad/cm

The dielectric constant ε is assumed constant. The quantity $dRdC$ which is equivalent to $\kappa\rho(x)$ has the dimension of time(sec) and can be denoted by τ

Therefore, we have

$$R_f=\frac{1}{\kappa A}\int_0^d \frac{\tau}{1+\omega^2\tau^2}\,dx \qquad (5)$$

$$\frac{1}{C_f}=\frac{1}{\kappa A}\int_0^d \frac{\omega^2\tau^2}{1+\omega^2\tau^2}\,dx \qquad (6)$$

Assuming an exponential dependence of resistivity on distance in the oxide, *i.e.*,

* Notation C_f and R_f denote properties of oxide films only whereas C_s and R_s denote properties of oxide films with external resistance. Refer to Eqs. (26), (27) and (28).

$\rho(x)=\rho_0 \exp(\alpha x)$ or $\tau=\tau_0 \exp(\alpha x)$ where ρ_o is the value at $x=0$, $\tau_o=\kappa\rho_o$ and α is constant. Young integrated Eqs. (5) and (6) and obtained the following results.

$$R_f=\frac{1}{\alpha\kappa A\omega}[\tan^{-1}(\omega\tau_d)-\tan^{-1}(\omega\tau_o)] \quad (7)$$

$$\frac{1}{C_f}=\frac{1}{2\alpha\kappa A}\ln\left(\frac{1+\omega^2\tau_d^2}{1+\omega^2\tau_o^2}\right) \quad (8)$$

where $\tau_d=\kappa\rho(d)=\tau_o \exp(\alpha d)$

Young further assumed that $\omega\tau_o\ll 1\ll\omega\tau_d$ in the audio frequency range. Then Eqs. (7) and (8) reduce to Eqs. (9) and (10).

$$R_f=\frac{1}{4C_o f\ln\frac{\tau_d}{\tau_o}} \quad (9)$$

$$\frac{1}{C_f}=\frac{\ln 2\pi\tau_d+\ln}{C_o\ln\frac{\tau_d}{\tau_o}} \quad (10)$$

where $C_o=\frac{\kappa A}{d}$

Equations (9) *and* (10) satisfied Young's experimental results. The further discussion of the equations is omitted bebause they are the special forms of the more general equations that are discussed subsequently.

Nishitani[1] suggested, as Scholte and van Geel[2] and Sasaki[3] did, the p-i-n structure of the films in which the distribution of resistivity ρ is not uniform. The concentration profiles of metal ions and oxygen ions are expected to be the usual diffusion layer profile which is approximated to be the reciprocal of exponential function as shown in Fig. 1. Since resistivity of the film is proportional to the

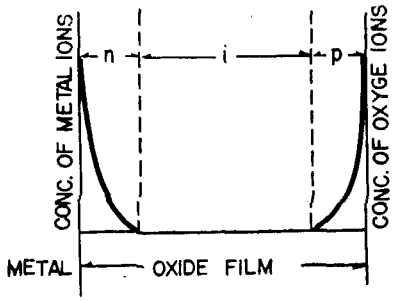

Fig. 1. Schematic p-i-n structure of anodic oxide film.

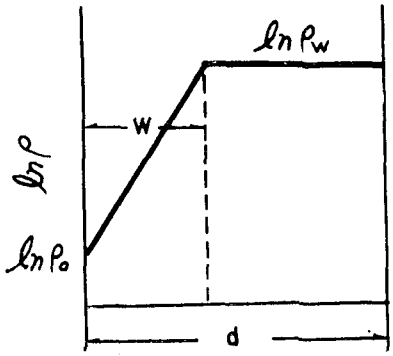

Fig. 2. The resistivity distribution in anodic oxide film.

reciprocal of the concentration of impurities, we have

$$0\le x\le w \qquad \tau=\tau_o \exp(\alpha x)$$
$$w\le x\le d \qquad \tau_w=\tau_o \exp(\alpha w) \quad (11)$$

where d and w are the total thickness of the oxide film and the total thickness of the diffusion layer, respectively, as shown in Fig. 2.

Substitution of Eq. (11) into Eqs. (5) and (6) gives us[1]

$$R_f=\left[\frac{\tan^{-1}\omega\tau_w-\tan^{-1}\omega\tau_o}{\omega\tau_w}+\frac{p\ln\frac{\tau_w}{\tau_o}}{1+(\omega\tau_w)^2}\right]\frac{\tau_w}{C_o(1+p)l_n\frac{\tau_w}{\tau_o}} \quad (12)$$

$$\frac{C_o}{C_f}=\frac{\ln\left[\frac{1+(\omega\tau_w)^2}{1+(\omega\tau_o)^2}\right]}{2(1+p)\ln\frac{\tau_w}{\tau_o}}+\frac{p(\omega\tau_w)^2}{(1+p)\{1+(\omega\tau_w)^2\}} \quad (13)$$

where $p=(d-w)/w$

If we introduce the condition of $\omega\tau_o\ll 1\ll\omega\tau_w$ as Young and Nishitani did, then we obtain the following equations;

$$R_f=\frac{\omega\tau_w\pi+2p\ln\frac{\tau_w}{\tau}}{2\omega^2C_o\tau_w(1+p)\ln\frac{\tau_w}{\tau_o}} \quad (14)$$

$$\frac{1}{C_f}=\frac{\ln\omega\tau_w+p\ln\frac{\tau_w}{\tau_o}}{C_0(1+p)\ln\frac{\tau_w}{\tau_o}} \quad (15)$$

$$\tan\delta_f=\omega C_f R_f=\frac{\omega\tau_w\pi+2p\ln\frac{\tau_w}{\tau_o}}{2\omega\tau_w\left(\ln\omega\tau_w+p\ln\frac{\tau_w}{\tau_o}\right)} \quad (16)$$

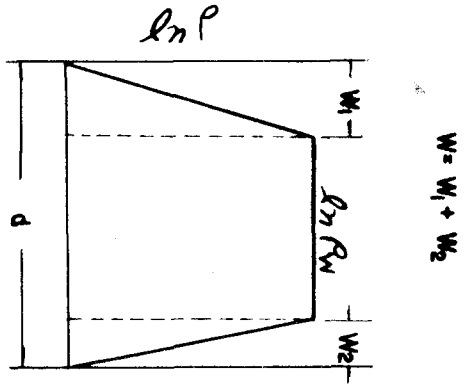

Fig. 3. The resistivity distribution in anodic oxide film.

For $\omega\tau_w$ to be 10 at 50 c/s, $\tau_w=0.0318$ sec, and for $\omega\tau_o$ to be 0.1 at 8Kc/s $\tau_o=1.99\times10^{-6}$ sec.

When p equals zero τ_w becomes τ_d, and Eqs. (14) and (15) reduce to Eqs. (9) and (10). The same results can be obtained for the case shown in Fig. 3.

If the capacitance C_{fo} at a given angular frequency ω_o is known, the capacitance C_f at arbitrary angular frequency ω is given by

$$\frac{C_{fo}}{C_f}=\frac{\ln\omega\tau_w+p\ln\frac{\tau_w}{\tau_o}}{\ln\omega_o\tau_w+p\ln\frac{\tau_w}{\tau_o}} \qquad (17)$$

Using Eqs. (17) and (16), Nishitani[1] expressed the experimental results on $\tan\delta_f$ and C_f in terms of parameters $p\log\frac{\tau_w}{\tau_o}$ and τ_w.

Nishitani however failed to evaluated parameter τ_o or p, and the parameters $p\log\frac{\tau_w}{\tau_o}$ and τ_w could not give clear physical picture of the model. In the following, methods of evaluating the parameters in Eqs. (14), (15) and (16) are presented. It can be seen by examining Eqs. (15) that plots of $\frac{1}{C_f}$ against $\log f$ are linear.

The slope is equal to $\frac{1}{C_o(1+p)\log\frac{\tau_w}{\tau_o}}$ (=slope) and the value of $\frac{1}{C_f}$ at $\log f=0$ is equal to

$$\frac{\log2\pi\tau_w+p\log\frac{\tau_w}{\tau_o}}{C_o(1+p)\log\frac{\tau_w}{\tau_o}}\ (=\text{intercept}) \qquad (18)$$

Hence, we obtain

$$\frac{\text{intercept}}{\text{slope}}=M=\log2\pi\tau_w+p\log\frac{\tau_w}{\tau_o} \qquad (19)$$

Substitution of Eq, (19) into Eq. (16) gives us the expression of $\tan\delta_f$ in terms of τ_w or $p\log\frac{\tau_w}{\tau_o}$. Therefore, values of $\tan\delta_f$ against frequency can be used to evaluate τ_w or $p\log\frac{\tau_w}{\tau_o}$. Once either τ_w or $p\log\frac{\tau_w}{\tau_o}$ is obtained, the other can be evaluated using Eq. (19). If we express $\tan\delta_f$ in terms of $p\log\frac{\tau_w}{\tau_o}$.

$$\tan\delta_f=\frac{\frac{\pi}{2}}{M\ln10+\ln f}+\frac{p\log\frac{\tau_w}{\tau_o}}{\omega\tau_w(M+\log f)} \qquad (20)$$

where $\tau_w=\frac{1}{2\pi}10^{\left(M-p\log\frac{\tau_w}{\tau_o}\right)}$ (21)

The value of M is obtained from the experimental data of C_f against frequency, the value of $p\log\frac{\tau_w}{\tau_o}$ can be evaluated from the measured data of $\tan\delta_f$ against frequency by the curve fitting, and the value of τ_w is calculated by making use of Eq. (21). Two unknown parameters that are to be evaluated are C_o and τ_o. However their unique values cannot be determined,

If we assume $\omega\tau_w\gg1$ and $\ln(1+\omega^2\tau_o^2)\ll1$, then Eqs. (12) and (13) reduce to Eqs. (22) and (23)

$$R_f=\left(\frac{\frac{\pi}{2}-\tan^{-1}\omega\tau_o}{\omega\tau_w}+\frac{p\ln\frac{\tau_w}{\tau_o}}{(\omega\tau_w)^2}\right)\cdot\left(\frac{\tau_w}{C_o(1+p)\ln\frac{\tau_w}{\tau_o}}\right) \qquad (22)$$

$$\frac{1}{C_f}=\frac{\ln\omega\tau_w+p\ln\frac{\tau_w}{\tau_o}}{C_o(1+p)\ln\frac{\tau_w}{\tau_o}} \qquad (23)$$

and $\tan\delta_f=\omega C_f R_f$

$$=\frac{\omega\tau_w\left(\frac{\pi}{2}-\tan^{-1}\omega\tau_o\right)+p\ln\frac{\tau_w}{\tau_o}}{\omega\tau_w\left(\ln\omega\tau_w+p\ln\frac{\tau_w}{\tau_o}\right)} \quad (24)$$

Note that Eq. (23) is the same as Eq. (15). The parameters in Eqs. (22) to (24) can be evaluated as follows; Substituting Eq. (19) into Eq. (24), we obtain

$$\tan\delta_f=\frac{\frac{\pi}{2}-\tan^{-1}\omega\tau_o}{M\ln 10+\ln f}+\frac{p\log\frac{\tau_w}{\tau_o}}{\omega\tau_w(M+\log f)} \quad (25)$$

where τ_w is given by Eq. (21). The values of τ_o and $p\log\frac{\tau_w}{\tau_o}$ can be evaluated from the experimental data of $\tan\delta_f$ against frequency. The value of τ_w is obtained by substituting the value of $p\log\frac{\tau_w}{\tau_o}$ into Eq. (21). Since the values of τ_w and τ_o are known, the value of p can be evaluated. Finally the value of C_o is obtained from Eq. (18) by substituting all the known values of parameters.

In order to demonstrate what is described above, electrical properties of an anodized tantalum foil before and after heat treatment will be analyzed and discussed based on the model subsequently.

3. Experimental Work

A tantalum foil of about 5 mil thickness was obtained by rolling 0.04" thick tantalum sheet of 99.95% purity obtained from Fansteel Metallurgical Corporation. A sample was cut from the 5 mil foil. The apparent surface area of the specimen was approximately 8cm^2. The sample was cut so that a 2 mm tab was left attached to serve as the electrical contact. The tab served the purpose of minimizing apparent area changes as the measuring electrolyte level changes. The sample was degreased in trichloro-ethylene and then polished in Bright Dip solution that is composed of 5 parts (by volume) of 98% H_2SO_4, 2 parts of 70% HNO_3, and 2 parts of 48% HF. The chemically polished sample was leached in the boiling deionized water for several minutes to remove residual fluoride. It was then vacuum annealed at 2000°C and 4×10^{-4}mm Hg for 30 min.

The sample was anodized in a 0.01% H_3PO_4 solution held at 90°C. The voltage was increased manually, maintaining a nearly constant formation current density less than 0.5 ma/cm^2 until 100 volt was reached. The sample was then held at the formation voltage for $1\frac{1}{2}$ hr.

Capacitance and dielectric loss measurements were made with GR Model 1608-A impedance bridge with GR 1310-B oscillator and GR 1232-A tunable detector, The bias voltage was not supplied, The measuring electrolyte was 30% H_2SO_4 at room temperature,

The heat treatment was carried out in air in a furnace controlled to ±10°C. The results obtained when the sample was heated at 260°C for 3 hours 50 minutes in air were compared with those obtained when the sample was not heated.

4. Results and Discussion

Experimental results are tabulated in Table 1 and 2. When anodized tantalum was heated at a temperature of 260°C for 2 hours 50 minutes, capacitance, tan δ_f and frequency dependences of equivalent series resistance and capacitance and capacitance all increased. Similar results have been reported previously by other investigators[5,6].

The measured values of equivalent series resistance R_s, equivalent series capacitance C_s and tan δ do not necessarily show characteristics of anodic oxide films. At low frequencies the measured values of C_s, R_s and tan δ are given as follows[7,8];

$$C_s=C_f \quad (26)$$

$$R_s=R_f+R_o \quad (27)$$

and $$\tan\delta=\tan\delta_f+\omega C_f R_o \quad (28)$$

where R_o is the external resistance due to

Table 1. Frequency characteristics of an anodized tantalum specimen before heating

Freq. (*Hz*)	1/Freq.	$C_s(\mu F)$	$1/C_s(\mu F^{-1})$	tan δ	tan δ_f	R_s(ohm)
25.	0.0400	1.4170	0.7057	0.005125	0.00508	23.0253
50.	0.0200	1.4140	0.7072	0.004850	0.00476	10.9180
100.	0.0100	1.4120	0.7082	0.004800	0.00445	5.4104
120.	0.0083	1.4110	0.7087	0.005280	0.00586	4.9630
200.	0.0050	1.4090	0.7097	0.004980	0.00428	2.8126
500.	0.0020	1.4050	0.7117	0.005750	0.00399	1.3027
1000.	0.0010	1.4020	0.7133	0.005400	0.00185	0.6130
2000.	0.0005	1.4000	0.7143	0.009000	0.0020	0.5116

R_o=0.4 ohm

Table 2. Frequency characteristics of an anodized tantalum after heating

Freq. (*Hz*)	1/Freq.	$C_s(\mu F)$	$1/C_s(\mu F^{-1})$	tan δ	tan δ_f	R_s(ohm)
50.	0.0200	1.5390	0.6398	0.043000	0.0354	88.9366
100.	0.0100	1.5200	0.6579	0.056700	0.0416	59.3690
120.	0.0083	1.5150	0.6601	0.052800	0.0348	46.2233
200.	0.0050	1.4990	0.6671	0.062000	0.0323	32.9140
500.	0.0020	1.4720	0.6793	0.101500	0.0284	21.9487
1000.	0.0010	1.4550	0.6873	0.168000	0.0235	18.3767
2000.	0.0005	1.4390	0.6949	0.308000	0.0225	17.0326

R_o=15.8 ohm

leads, electrodes, electroyte, *etc*, whose value is the equivalent series resistance intercepted at $1/f=0$ in plots of the equivalent series resistance against $1/f$. The external resistance of an anodized tantalum specimen before and after heating was found to be 0.4 and 15.8 ohms. The substantial increase in resistance R_o after heating is attributed to a local short-circuiting of the Ta_2O_5 film due to extraction of some of the oxygen from the oxide film by the tantalum. Figure 4 shows experimental plots of $1/C_f$ against log f.

As expected from Eq. (15) (23), plots of $1/C_f$ *vs.* log f show linear dependence. Plots of $\tan\delta_f$ *vs.* frequency and R_f *vs.* frequency are shown in Figs. 5 and 6, respectively.

Substantial changes in frequency characteristics of C_f, tan δ_f and R_f due to heating the specimen can be explained by examining the values of parameters in Table 3, which satisfy the assumptions we made in the derivation of

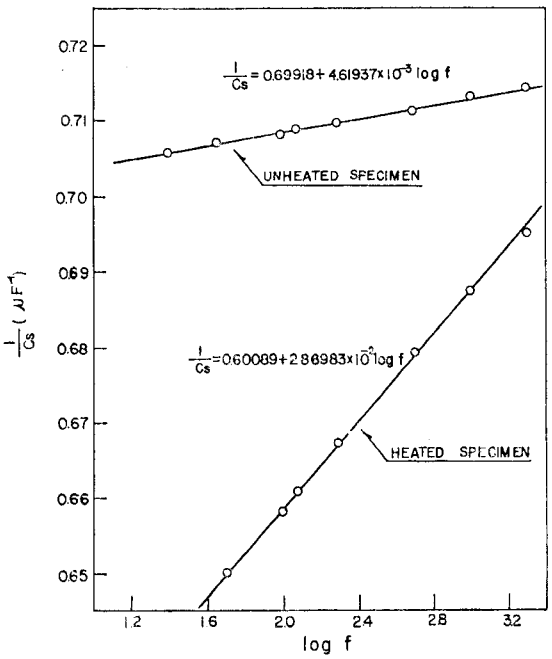

Fig. 4. Plots of $1/C_s$ *vs.* log f.

Eqs. (22) to (24) in the frequency ranges between a lower range of audio frequency and

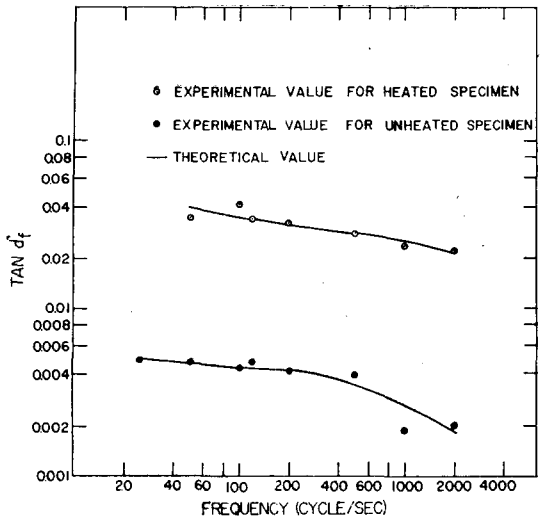

Fig. 5. Plots of tan δ_f *vs.* frequency.

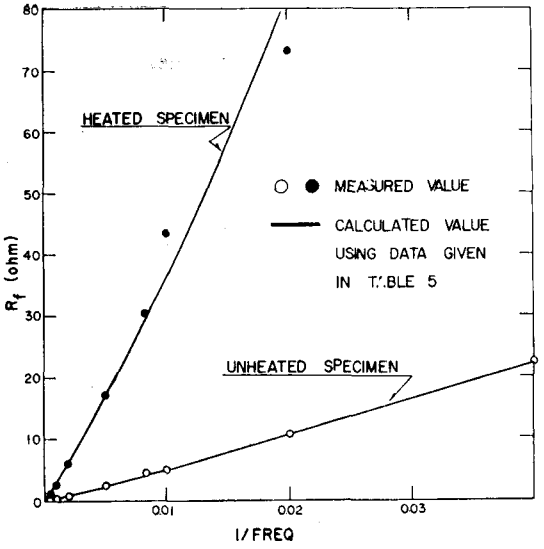

Fig. 6. Plots of R_f *vs.* frequency.

several thousand hertz. The values of parameters are shown in Fig. 7. A substantial increase in diffusion layer due to heat treatment may be expected. A decrease in resistivity of the anodic oxide film may be attributed to either a change in the crystallinity of the tantalum oxide film[10, 11] or to cracks in the film or to the both effects. Anyhow an increase in the leakage current was observed for the specimen heat-treated(our unpublished results).

It is also noted that the values in Table 3 show the assumption, $\omega\tau_w \gg 1$, in the audio frequency range, whereas the assumption, $\omega\tau_o \ll 1$, holds only in a rather low frequency range. The various properties of anodic oxide films will be discussed based on Eqs. (23), (24) in our forthcoming paper[13].

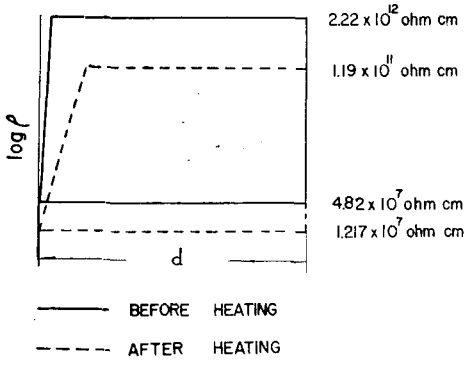

Fig. 7. Changes in the resistivity distribution before and after heat-teatment.

Table 3. Changes in characteristics of the anodic oxide film by heat treatment: Analyzed using Eqs. (23) and (24)

characteristics of an anodized tantalum specimen before heating		Characteristics of an anodized tantalum specimen after heating
τ_w	5.42 sec	0.291 sec
ρ_w	2.22×10^{12} ohm cm	1.19×10^{11} ohm cm
τ_o	1.176×10^{-4} sec	2.972×10^{-5} sec
ρ_o	4.82×10^{7} ohm cm	1.217×10^{7} ohm cm
C_o	1.400 μF	1.412 μF
p	32.1	5.18
$p\log(\tau_w/\tau_o)$	149.67	20.67

5. Summary

A method is presented for evaluating parameters in the equations for impedance of anodic oxide films that were derived based on a p-i-n model. The model is then used to explain the changes in frequency dependence of the impedance of equivalent series capacitance and equivalent series resistance when the specimen is heated. These changes are attributed to the increases in the diffusion layer and to the increase in the conductivity of the film.

Acknowledgments

The authors wish to thank Dr. K. Nishitani of Hitachi, Ltd. at Yokohama Research Laboratory for his critical comments and Mr. Heon Yi Kim for his assistance with experiments.

References

1) K. Nishitani, J. I. E. E. E. J. **88**, 2071 (1968)
2) J. W. A. Scholte and W. Ch. van Geel, Philips Res. Rep. **8**, 47 (1953)
3) Y. Sasaki, J. Phys. Chem. Solids **13**, 177 (1960)
4) L. Young, Trans. Faraday Soc. **51**, 1250(1955)
5) D. M. Smyth, G. A. Shirn and T. B. Tripp, J. Electrochem, Soc. **110** (12), 1264 (1963)
6) D. A. Vermilyea, Acta Met. **5**, 113 (1957)
7) D. A. McLean, J. Electrochem. Soc. **108**, 48 (1961)
8) K. Nishitani, J. I. E. E. J. **89**, 1333 (1969)
9) L. Young, Anodic Oxide Films(Academic Press, London and New York, 1961)
10) D. A. Vermilyea, J. Electrochem. Soc. **104**, 485 (1957)
11) L. D. Calvert and P. H. G. Draper, Can. J. Chem. **40**, 1943 (1962)
12) D. N. Lee and Y. K. Yoon, J. Korean Inst. Metals **10** 147 (1972)
13) D. N. Lee and Y. K. Yoon, Frequency Characteristics of Anodic Oxide Films, to be published